Monthly Notices
of the
ROYAL ASTRONOMICAL SOCIETY

MNRAS **441,** 739–744 (2014) doi:10.1093/mnras/stu607

CCD photometry of distant active comets 228P/LINEAR, C/2006 S3 (LONEOS) and 29P/Schwassmann–Wachmann 1

J. C. Shi,[1,2]★ Y. H. Ma[1,2] and J. Q. Zheng[3]

[1]*Purple Mountain Observatory, Chinese Academy of Sciences, Nanjing 210008, China*
[2]*Key Laboratory of Planetary Sciences, Chinese Academy of Sciences, Nanjing 210008, China*
[3]*Tuorla Observatory, FI-21500 Piikkio, Finland*

Accepted 2014 March 25. Received 2014 February 18; in original form 2013 December 18

ABSTRACT

We presentphotometric investigations of three distant active comets, 228P/LINEAR, C/2006 S3 Lowell Observatory Near-Earth-Object Search (LONEOS) and 29P/Schwassmann–Wachmann 1. The data were obtained with the 1-m optical telescope at Lulin Observatory in Taiwan on 2011 February 5 and 6. These comets were observed at heliocentric distances larger than 3 au, all of them appeared to be active. By cometary morphological and photometric studies, the upper limits of the nuclei radii were derived. Also, the surface brightness profiles, $Af\rho$ parameters, mass production rates and the coma colours were measured. Finally, we discussed possible driver of activity in comets.

Key words: techniques: photometric – comets: general.

1 INTRODUCTION

Generally, a comet at a large distance from the Sun is supposed to be inactive due to the low temperature and the absence of gas sublimation leading to coma formation. But it is known from observations that the activity of comets far from the Sun is common (Luu 1993; Lamy et al. 2004; Meech & Svoren 2004; Mazzotta Epifani et al. 2007, 2008, 2009, 2010, 2011; Korsun, Ivanova & Afanasiev 2008; Snodgrass, Lowry & Fitzsimmons 2008; Ivanova, Korsun & Afanasiev 2009; Jewitt 2009). Meech & Hainaut (2001) discussed the importance of observing distant comets in investigating the processes of formation and evolution of planetesimals.

The primary driver of activity in comets close to the Sun is sublimation of water ice and can be explained by the standard model (Whipple 1950). Beyond a heliocentric distance of 3 au, the sublimation rate for water ice decreases significantly. Though activity is lower, water ice sublimation driven activity is still measurable out to 5–6 au (Meech & Jewitt 1986). Beyond this distance, the activity of comets must be explained by other mechanisms. Ivanova et al. (2011) summarized various mechanisms to explain the nucleus activity at large heliocentric distances. These are the sublimation of more volatile admixtures, such as CO and/or CO_2 ice (Houpis & Mendis 1981; Luu 1993); polymerization of HCN (Rettig 1992); crystallization of the amorphous water ice (Prialnik 1992; Gronkowski & Smela 1998) and annealing of the amorphous water ice (Meech et al. 2009).

The objects of our observation are comets at heliocentric distances larger than 3 au. By the observations, we aimed to investigate the physical properties and activities of distant comets 228P/LINEAR, C/2006 S3 Lowell Observatory Near-Earth-Object Search (LONEOS) and 29P/Schwassmann–Wachmann 1.

Object 228P/LINEAR is not really a 'distant' object, but results for this comet are interesting and the data are relatively scarce. It was first discovered by the LINEAR monitoring telescope on 2001 December 17, and designated P/2001 YX_127 (LINEAR) (Green 2002). The comet was recovered by J. Scotti with the Spacewatch II telescope at Kitt Peak on 2009 October 18, it was very slightly diffuse, with a short but faint tail (Green 2009a).The permanent number 228P has been assigned to comet P/2009 U2 = P/2001 YX_127 on 2009 November 11 (Green 2009b).

Object C/2006 S3 (LONEOS) was discovered on 2006 September 19 at a heliocentric distance of 14.29 au by the LONEOS programme based in Flagstaff, Arizona. It presented a diffuse 10 arcsec coma, which was elongated towards the east, but showed no tail (Green 2006). The comet passed its perihelion on 2012 April 16.

Object 29P/Schwassmann–Wachmann 1 was discovered on 1927 November 15 by Arnold Schwassmann and Arno Arthur Wachmann at the Hamburg Observatory in Bergedorf, Germany. Jewitt (1990) noted that the coma of 29P/Schwassmann–Wachmann 1 never disappeared completely since its discovery. Trigo-Rodriguez et al. (2008, 2010) found a clear periodicity of 50 d based on the outbursts recorded from 2002 to 2010. But it is still impossible to predict the time of outburst.

In this paper, we present the results of data processing, the upper limits of the nuclei radii, the surface brightness profiles, the dust production and mass production rates and the colour index.

2 OBSERVATIONS AND DATA PROCESSING

Our observations were carried out with the 1-m optical telescope at Lulin Observatory in Taiwan. Imaging data were obtained with

★ E-mail: jcshi@pmo.ac.cn

Table 1. Log of all observations.

Comet	q (au)	UT date	R_h(au)	Δ(au)	$\alpha(^\circ)$	$N_{exp}\times$ filter	t_{exp}(s)
228P/LINEAR	3.428	2011-04-05	3.474^I	3.321	16.7	$9\times B, 9\times V, 9\times R$	60
		2011-04-06	3.473^I	3.334	16.7	$10\times B, 10\times V, 10\times R$	60
C/2006 S3	5.131	2011-04-05	5.860^I	6.167	9.1	$7\times B, 7\times V, 7\times R$	60
(LONEOS)		2011-04-06	5.857^I	6.147	9.2	$15\times B, 14\times V, 14\times R$	60
29P/Schwassmann–	5.743	2011-04-05	6.253^O	5.390	5.0	$28\times B, 28\times V, 28\times R$	60
Wachmann 1		2011-04-06	6.253^O	5.398	5.1	$19\times B, 19\times V, 19\times R$	60

Note. q is the perihelion distance; R_h is the heliocentric distance in au; superscripts 'I' and 'O' refer to whether the comet is inbound (pre-perihelion) or outbound (post-perihelion); Δ is the geocentric distance in au; α is the solar phase angle in degrees; and t_{exp} is the total exposure time in seconds.

an Alta U42 2k × 2k CCD camera. The camera had a pixel scale of 0.348 arcsec and a field of view (FOV) of 11.9 × 11.9 arcmin^2. Conditions were excellent and both two nights were photometric. The seeing measured in the images on the first night varied between 1.0 and 1.4 arcsec, with an average of 1.1 arcsec. The seeing measured that in the images on the second night varied between 1.1 and 1.9 arcsec, with an average of 1.1 arcsec.

The images of comets were collected through Asahi broad-band *B*, *V*, *R* filters and in a sequence of *BVR,...,BVR*. The *B* filter has the effective wavelength $\lambda_e = 4405$ Å and full width at half-maximum (FWHM) of $\Delta\lambda = 1160$ Å, the *V* filter has $\lambda_e = 5400$ Å and $\Delta\lambda = 850$ Å, the *R* filter has $\lambda_e = 6578$ Å and $\Delta\lambda = 1215$ Å. During the observations, the telescope was set to track the sidereal motion, with exposure times chosen so that the apparent motion of the comet would be less than 0.4 arcsec, and would thus remain within the seeing disc. The log of all observations is listed in Table 1.

Standard bias subtraction, flat-field correction and cleaning from cosmic ray tracks were performed on all images. The bias value was obtained from an average of several zero-exposure frames. Flat-fields were constructed from dithered images of the twilight sky. To avoid the contaminating effects of the coma, we chose the region far from the nucleus as background sky statistics which was used for photometry in the IRAF task PHOT. To provide absolute photometric calibration, we observed the Landolt photometric standard stars PG1047, PG1323 and SA104. These stars were taken throughout the night. Using the IRAF package PHOTCAL, Landolt standard star measurements gave the zero-point, extinction coefficient and colour term for each filter for each night. These were then used to calculate the magnitudes of the field stars in each frame. Taking the mean of these values gave us a very accurate measurement of the brightness of our comparison stars. Adding this value to each of the differential comet magnitudes gave us accurate calibrated comet magnitudes.

3 COMET MORPHOLOGY

Despite the large heliocentric distance at the time of observation, comets 228P/Linear, C/2006 S3 (LONEOS) and 29P/Schwassmann–Wachmann 1 were easily identifiable and appeared active in every single exposure. To increase the signal-to-noise ratio for the image analysis, we decided to co-add the *B*, *V* and *R* images in order to obtain three 'final' images for each filter. We selected the co-added images of comets observed through *R* filter on April 6 (the first column of Fig. 1) as one representative image and profile for each comet, since there is no obvious morphological difference between filters and between the two nights of observation. Co-added *R*-band images of the comets were analysed using a radial normalization method (Birkle & Boehnhardt 1992) to reveal possible structures inside the coma (the second column of Fig. 1). Comet 228P/LINEAR shows a fan-like structure in the south-east quadrant. Comet C/2006 S3 (LONEOS) shows a fan-like structure in the north-east quadrant. For 29P/Schwassmann–Wachmann 1, there is a fan-like structure in the north-east quadrant and three jets emanating from the nucleus and curving right, this is consistent with the nucleus having an anticlockwise rotation as viewed from *Spitzer* (Stansberry et al. 2004).

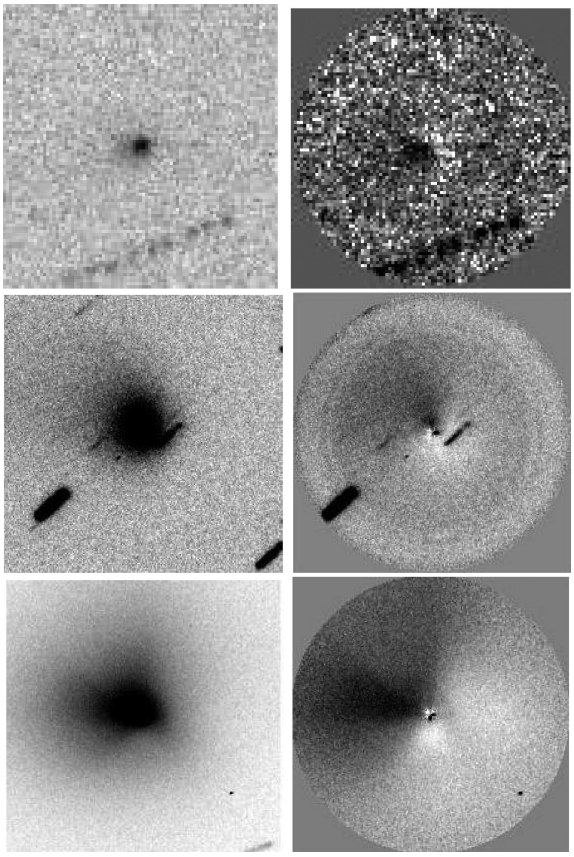

Figure 1. Coma structures of comets 228P/LINEAR (top), C/2006 S3 (LONEOS) (middle) and 29P/Schwassmann–Wachmann 1 (bottom) in the *R* filter on 2011 April 6. First column shows co-added images, second column shows radial renormalization enhancement of the final images. All images are oriented north-up, east-left. The FOV of 228P/LINEAR is 0.53 × 0.53 arcmin^2. The FOVs of C/2006 S3 (LONEOS) and 29P/Schwassmann–Wachmann 1 are 1.29 × 1.29 arcmin^2. The scales of the processed images are the same as those of the unprocessed images.

4 PHOTOMETRY

4.1 Nucleus size

The photometric R magnitude, m_R, can be used to estimate the upper limit of the geometric cross-section of the cometary nucleus, using the expression of Russell (1916) derived for asteroids observed at large phase angle, which, in the case of a spherical object, is given by

$$A_R a_N^2 < 2.24 \times 10^{22} R_h^2 \Delta^2 10^{0.4(m_\odot - m_R + \beta\alpha)}, \quad (1)$$

where $A_R = 0.04$ (Lamy et al. 2004) is the geometric albedo, a_N is the radius of the target in (m), R_h is the heliocentric distance in (au), Δ is the geocentric distance in (au), $m_\odot = -27.10$ (Holmberg, Flynn & Portinari 2006) is the magnitude of the Sun in the same wavelength band as the observations, α is the phase angle in (°), $\beta = 0.035$ (Lamy et al. 2004) is the phase coefficient (mag deg^{-1}). An analogous stack that aligns the field stars instead of the comet was used to investigate the best choice of aperture for the photometry. The radius of the photometry aperture is the star's FWHM in these co-added images that aligns the field stars. From the equation (1), we obtain the upper limit of the nucleus radius of comet 228P/LINEAR is $a_N < 4.05$ km and the average R magnitude is $m_R = 20.127 \pm 0.018$; for comet C/2006 S3 (LONEOS), $a_N < 35.75$ km and $m_R = 17.613 \pm 0.008$; for comet 29P/Schwassmann–Wachmann 1, $a_N < 36.25$ km and $m_R = 17.291 \pm 0.008$.

4.2 Surface brightness profiles

The surface brightness profiles of the comets are presented in Fig. 2. Diagonal lines indicate a gradient $m = \frac{d\log B}{d\log \rho}$, where $m = -1$ represents a symmetric steady-state coma model, and $m = -1.5$ represents a solar radiation pressure model. The profiles of comet 228P/LINEAR shows the gradient approaching $m = -1.5$. The profile of comets C/2006 S3 (LONEOS) and 29P/Schwassmann–Wachmann 1 can be divided into two parts, the inner part has a steep brightness gradient, this can be explained as 'acceleration zone' (Jewitt & Meech 1987), in which the grains are accelerated to terminal velocity around the nucleus and the grain number density should deviate from the inverse square law. The outer part has the gradient approaching $m = -1.5$.

4.3 $Af\rho$ and mass production rate

The $Af\rho$ value (cm; A'Hearn et al. 1984), is usually used as a proxy for the cometary dust production, and can be estimated using the formalism

$$Af\rho = \frac{4R_h^2\Delta^2 10^{0.4(m_\odot - m_C)}}{\rho}, \quad (2)$$

where A is the average grain albedo, f is the ratio of the cross-section of the dust grains to the total FOV, ρ is the projected radius of the photometric aperture in (cm), $m_\odot$ is the solar magnitude in the same band, m_C is the comet integrated magnitude calculated for the aperture of radius ρ. When the cometary coma is in a steady state, $Af\rho$ is an aperture-independent parameter. To determine the radius at which the $Af\rho$ value is begin constant, we calculated the $Af\rho$ parameter for different values of the aperture radius.

The multi-aperture $Af\rho$ values in R band show that the $Af\rho$ values of comet 228P/LINEAR on 2011 April 5 increase suddenly outside 3.2 arcsec, this is caused by nearby stellar contamination. For comet 228P/LINEAR on 2011 April 6 outside 1.7 arcsec and for comet C/2006 S3 (LONEOS) on 2011 April 5 and 6 outside 3.13 arcsec, the $Af\rho$ is constant (within the error bars), so depicting a dust environment consistent with a scenario of steady-state emission. But for comet 29P/Schwassmann–Wachmann 1 on both nights, the multi-aperture $Af\rho$ values show that the $Af\rho$ is bulge first then dip, which may indicate a non-steady-state dust emission.

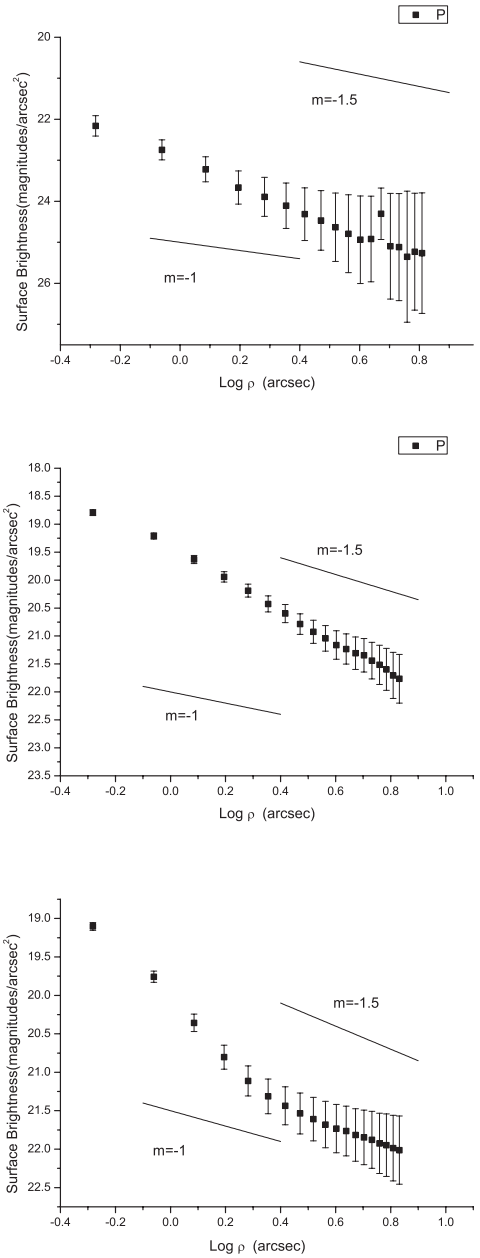

Figure 2. Surface brightness profiles of comets 228P/LINEAR (top), C/2006 S3 (LONEOS) (middle) and 29P/Schwassmann–Wachmann 1 (bottom) in the R filter on 2011 April 6.

The coma integrated magnitudes, derived for all the filters in a circular aperture of $\rho = 5$ arcsec and the $Af\rho$ values in R band are summarized in Table 2.

Dust production rate can then be used to estimate mass-loss rate Q_{dust}. The formalism is presented by Meech & Weaver (1996)

$$Q_{dust} = \frac{Af\rho(4a_{dust}v_{ej}\sigma)}{3p}, \quad (3)$$

Table 2. Coma magnitude, colours and $Af\rho$ at reference aperture of $\phi = 5$ arcsec.

Comets	ρ (10^5 km)	B band (mag)	V band (mag)	R band (mag)	$B-V$	$V-R$	$Af\rho$ (cm)
228P/LINEAR							
April 5	6.90	19.42 ± 0.03	18.58 ± 0.02	18.26 ± 0.01	0.84 ± 0.04	0.32 ± 0.02	71.4 ± 2.1
April 6	6.93	20.42 ± 0.06	19.64 ± 0.04	18.78 ± 0.02	0.78 ± 0.07	0.83 ± 0.04	44.0 ± 2.3
C/2006 S3 (LONEOS)							
April 5	12.81	17.21 ± 0.01	16.50 ± 0.01	16.06 ± 0.01	0.71 ± 0.01	0.44 ± 0.01	2846.1 ± 54.5
April 6	12.77	17.00 ± 0.01	16.38 ± 0.01	15.97 ± 0.01	0.62 ± 0.01	0.41 ± 0.01	3082.6 ± 43.2
29P/Schwassmann–Wachmann 1							
April 5	11.20	17.16 ± 0.01	16.27 ± 0.01	15.79 ± 0.01	0.89 ± 0.01	0.48 ± 0.01	3617.6 ± 57.4
April 6	11.22	17.03 ± 0.01	16.25 ± 0.01	15.77 ± 0.01	0.78 ± 0.01	0.48 ± 0.01	3713.1 ± 70.6

Note. ρ is linear radius at reference aperture of $\phi = 5$ arcsec and $Af\rho$ is obtained in the R band.

where $a_{\rm dust}$ is a mean dust grains radius, p is the geometric albedo of the dust grains, σ is grain density and $v_{\rm ej}$ is the grain ejection velocity.

Expansion measurements for comet Hale–Bopp in the range $4 \leq r \leq 14$ au infer that the radial outflow speed of dust grains from the nucleus is $v(r) = v_0(r_0/r)^{1/4}$, where $v_0 = 550$ m s^{-1} and $r_0 = 5$ au (Biver et al. 2002). Probstein's theory (Probstein 1969; Fulle, Cremonese & Bhm 1998) predicts, for spherical grains emitted from a perfectly homogeneous nucleus, a dust velocity is close to 10 per cent of the gas value. Since the Hale–Bopp measurements refer to gas, we adopt a more realistic dust grain ejection velocity $v_{\rm ej} = v(r)/10$.

The dust size distribution, which a good approximation is obtained by setting a power-law distribution with $q = 3.5$ in a dust grain size range between $a_- = 0.1$ μm and $a_+ = 1$ cm (Grün et al. 2001). To calculate the dust production rate, we took dust particle radius value of $a_{\rm dust}$ equal to the size of the average dust grain $(a_- a_+)^{1/2} \simeq 30$ μm.

For the dust grain albedo, we assume $p = 0.04$. For the density of the grain material, based on systematic experiments, Niimi et al. (2012) estimated that the average density of the entire sample was $\sigma = 0.49 \pm 0.18$ g cm^{-3}, the sample was collected from comet 81P/Wild 2 and returned to Earth by the NASA Stardust mission (Brownlee et al. 2006).

Using equations (2) and (3), we estimated the dust mass production rate of comets. For comet 228P/LINEAR, the mass-loss rate $Q_{\rm dust}$ equals 11.2 kg s^{-1} on 2011 April 5 and 6.9 kg s^{-1} on 2011 April 6, respectively. For comet C/2006 S3 (LONEOS), $Q_{\rm dust}$ equals 345.7 kg s^{-1} on 2011 April 5 and 374.5 kg s^{-1} on 2011 April 6, respectively. For comet 29P/Schwassmann–Wachmann 1, $Q_{\rm dust}$ equals 425.4 kg s^{-1} on 2011 April 5 and 436.6 kg s^{-1} on 2011 April 6, respectively.

The variation of the $Af\rho$ parameter and mass production rate mostly mean the variation of the activity of comets at different epoch. But for comet 228P/LINEAR observed on 2011 April 5 the variation is caused by nearby stellar contamination, we use the data observed on 2011 April 6 only to do analyses hereafter.

4.4 Coma colour

The data obtained during the observations allow us to perform an analysis of the coma colour. Table 2 summarizes the coma B, V, R magnitude and colour at reference aperture of $\phi = 5$ arcsec. The temporal variations of the $B-V$ and $V-R$ colours greater than the photometric uncertainty may be attributed to intrinsic variations

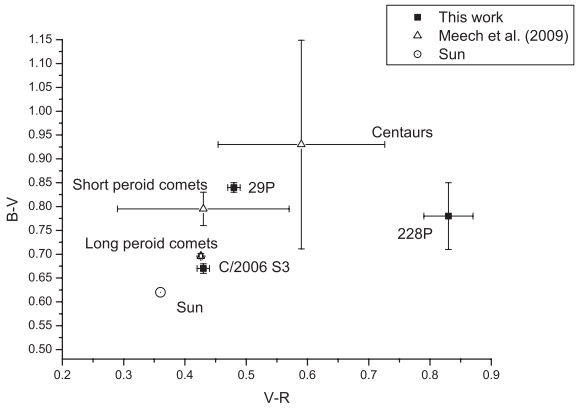

Figure 3. $B-V$ colour plotted against $V-R$ colour for this work (filled square) and other work (triangles). The colour of the Sun is marked (⊙).

of the coma properties (e.g. composition, dust size distribution) coupled with different observing conditions (Mazzotta Epifani et al. 2011).

Fig. 3 shows broad-band colours $B-V$ versus $V-R$ diagram. The data of this work (filled square) are taken from the average colour indices of Table 2, the solar colour indices (⊙) used here are $B-V = 0.62$ and $V-R = 0.36$ (Drilling & Landolt 2000), while other data (triangles) are taken from table 6 of Meech et al. (2009). Fig. 3 suggests a trend of increasing $(B-V)$ with increasing $(V-R)$, implying that the albedo of these nuclei continues to rise through the B, V and R bands. Comparing the coma colour indices we obtained with the solar colour indices, we find that the colours of all three comets are redder than that of the Sun. Comet 228P/Linear is a short-period comet (SP), its colour indices is in the error bars range of average colour indices of SP in $B-V$ but not in $V-R$. Comet C/2006 S3 (LONEOS) is a long-period comet (LP), its colour indices is closer to average colour indices of LP. Comet 29P/ Schwassmann–Wachmann 1 is a Centaur, its colour indices is in the error bars range of average colour indices of Centaur.

5 DISCUSSION

Generally, the values of $Af\rho$ vary within the range between 5 and 5000 cm and are mainly affected by the size of the comet and its distance from the Sun. Comparing the values of $Af\rho$ for all three comets, we find that the activity of comet 228P/LINEAR is much lower than other two comets, which can be explained by the smaller

Table 3. Summary of available broad-band photometry results of comet 29P/Schwassmann–Wachmann 1.

R_h(au)	$Af\rho$(cm)	Q_{dust} (kg s^{-1})	$B-V$	$V-R$	Number of jets	Reference
6.253^O	3665.4	431.0	0.84 ± 0.01	0.48 ± 0.01	3	This work
5.865^O	1168					Ivanova et al. (2011)
6.118^O	890					Ivanova et al. (2011)
5.865^O	7325	365	0.64 ± 0.09	0.54 ± 0.08		Ivanova et al. (2009)
5.967^O	4637	182			2–3	Ivanova et al. (2009)
5.919^I	16600					Szabo et al. (2002)
5.810^I			0.78 ± 0.03	0.50 ± 0.03		Jewitt (2009)
			0.8			Hartmann, Cruikshank & Dejewij (1982)
5.886^I				0.502		Meech et al. (1993)
5.822^I		10				Jewitt (1990)
5.772^P		600 ± 300				Fulle (1992)
5.724^P		300 ± 100				Moreno (2009)
5.865^O					5–6	Korsun et al. (2008)
6.067^O					4–5	Trigo-Rodriguez et al. (2010)
6.192^O	5000–56 000^b					Trigo-Rodriguez et al. (2010)
6.254^O	2700–20 000^b	22–500				Hosek et al. (2013)
6.255^I	2000–12 500^b	16–300				Hosek et al. (2013)

Note. Superscripts 'I' refer to the comet is inbound (pre-perihelion), 'O' refer to the comet is outbound (post-perihelion),'P' refer to the comet is at perihelion, '^{b}' refer to the comet outburst.

size of the comet. Comparing comet C/2006 S3 (LONEOS) with 29P/Schwassmann–Wachmann 1, we find that though the comet 29P/Schwassmann–Wachmann 1 has the same upper limit of the nucleus size and larger distance from the Sun than the comet C/2006 S3 (LONEOS), the activity is higher than C/2006 S3 (LONEOS), which may be indicated the composition difference between two comets.

As there are no publications about comets 228P/LINEAR and C/2006 S3 (LONEOS) at present, we cannot compare the physical properties and activity for these comets with observational data of other observers.

For comet 29P/Schwassmann–Wachmann 1, Meech et al. (1993) summarized the radius of the nucleus lies in the range of 15–44 km as obtained from visual photometry, Stansberry et al. (2004) obtained the nuclear radius is 27 ± 5 km from the analysis of its thermal emission in 2003 November; our value for the upper limit of the nucleus radius lies in this range.

Table 3 summarizes available broad-band photometry results of comet 29P/Schwassmann–Wachmann 1 up to present. From Table 3, we can find that the variation of the $Af\rho$ parameter may be connected with variations in the number of jets. Hosek et al. (2013) obtained that the average quiescent dust production of 29P/Schwassmann–Wachmann 1 is around $Af\rho = 2000$ cm, our value is higher than 2000 cm which indicates the comet is during an outburst phase. Senay & Jewitt (1994) and Crovisier et al. (1995) inferred a CO production rate of ∼2000 kg s^{-1} in comet 29P/Schwassmann–Wachmann 1. The CO production rate exceeds even the larger estimates of dust production, showing that CO is an important driver of activity in comet 29P/Schwassmann–Wachmann 1.

Comet 228P/LINEAR is a Jupiter Family Comet, whose primary driver of activity is sublimation of water ice. Though it was observed at a heliocentric distance of 3.47 au and activity is lower, water ice sublimation driven activity is still possible. For comets C/2006 S3 (LONEOS), it was observed at a heliocentric distance larger than 5 au, water ice sublimation driven activity is impossible, CO sublimation driven activity is a possible mechanism, but we need more observation data to affirm it. Comparing with water ice driven activity, Mazzotta Epifani et al. (2009) concluded that CO and its associated dust flux are expected to leave the comet nucleus uniformly from all the nucleus surface, its loss rate should be changed very slowly with time after the onset of activity since the source of a CO-driven activity originates from the nucleus interior.

6 CONCLUSIONS

Our observations reveal the activity and physical properties of comet 228P/LINEAR, C/2006 S3 (LONEOS) and 29P/Schwassmann–Wachmann 1 at larger heliocentric distance, including the following:

(i) Comets 228P/Linear, C/2006 S3 (LONEOS) and 29P/Schwassmann–Wachmann 1 were observed to be active at heliocentric distances larger than 3 au.

(ii) The surface brightness profiles of the comets show that all three comets can be explained by a solar radiation pressure model.

(iii) Dust production and mass production rates of three comets were estimated. $Af\rho$ and Q_{dust} of comet 228P/LINEAR were about 44 cm and 6.9 kg s^{-1}, respectively. $Af\rho$ and Q_{dust} of comet C/2006 S3 (LONEOS) were about 2964.4 cm and 360.1 kg s^{-1}, respectively. $Af\rho$ and Q_{dust} of comet 29P/Schwassmann–Wachmann 1 were about 3665.4 cm and 431.0 kg s^{-1}, respectively. The results demonstrate that 228P/LINEAR has a lower activity, while C/2006 S3 (LONEOS) and 29P/Schwassmann–Wachmann 1 have higher activity even at large heliocentric distances.

(iv) The coma colour indices of comet 228P/LINEAR are $B-V = 0.78 \pm 0.07$ and $V-R = 0.83 \pm 0.04$. The average coma colour index of comet C/2006 S3 (LONEOS) are $B-V = 0.67 \pm 0.01$ and $V-R = 0.43 \pm 0.01$. The average coma colour indices of comet 29P/Schwassmann–Wachmann 1 are $B-V = 0.84 \pm 0.01$ and $V-R = 0.48 \pm 0.01$.

(v) For comet 228P/LINEAR, water ice sublimation driven activity is possible. For comet 29P/Schwassmann–Wachmann 1, activity could be explained by the sublimation or the release of CO and/or CO_2. For comet C/2006 S3 (LONEOS), CO sublimation driven activity is a possible mechanism, but more observation data are needed.

ACKNOWLEDGEMENTS

This work was based on observations obtained at Lulin Observatory whose staff and assistants kindly helped us to finish these observations. We thank David Jewitt for discussions about the manuscript. We acknowledge the support of the National Natural Science Foundation of China (Grant nos. 11003048, and 10933004), CAS Oversea Study & Training Program, Minor Planet Foundation of Purple Mountain Observatory and the exchange program between Finnish Academy (FA) and NSFC.

REFERENCES

A'Hearn M. F., Schleicher D. G., Feldman P. D., Millis R. L., Thompson D. T., 1984, AJ, 89, 579
Birkle K., Boehnhardt H., 1992, Earth Moon Planets, 57, 191
Biver N. et al., 2002, Earth Moon Planets, 90, 5
Brownlee D. et al., 2006, Science, 314, 1711
Crovisier J., Biver N., Bockelee-Morvan D., Colom P., Jorda L., Lellouch E., Paubert G., Despois D., 1995, Icarus, 115, 213
Drilling J. S., Landolt A. U., 2000, in Cox A. N., ed., Allen's Astrophysical Quantities. Springer, New York
Fulle M., 1992, Nature, 359, 42
Fulle M., Cremonese G., Böhm C., 1998, ApJ, 116, 1470
Green D. W. E., 2002, IAU Circ., 7828
Green D. W. E., 2006, IAU Circ., 8752
Green D. W. E., 2009a, IAU Circ., 9085
Green D. W. E., 2009b, IAU Circ., 9094
Gronkowski P., Smela J., 1998, A&A, 338, 761
Grün E. et al., 2001, A&A, 377, 1098
Hartmann W. K., Cruikshank D. P., Dejewij J., 1982, Icarus, 52, 377
Holmberg J., Flynn C., Portinari L., 2006, MNRAS, 367, 449
Hosek M. W., Jr, Blaauw R. C., Cooke W. J., Suggs R. M., 2013, AJ, 145, 122
Houpis H. L. F., Mendis D. A., 1981, Moon Planets, 25, 397
Ivanova A. V., Korsun P. P., Afanasiev V. L., 2009, Sol. Syst. Res., 43, 453
Ivanova O. V., Skorov Y. V., Korsun P. P., Afanasiev V. L., Blum J., 2011, Icarus, 211, 559
Jewitt D., 1990, ApJ, 351, 277
Jewitt D., 2009, ApJ, 137, 4296
Jewitt D., Meech K. J., 1987, ApJ, 317, 992
Korsun P. P., Ivanova O. V., Afanasiev V. L., 2008, Icarus, 198, 465
Lamy P. L., Toth I., Fernandez Y. R., Weaver H. A., 2004, in Festou M. C., Keller H. U., Weaver H. A., eds, Comets II, The Sizes, Shapes, Albedos, and Colors of Cometary Nuclei. Univ. Arizona Press, Tucson, AZ, p. 223
Luu J. X., 1993, PASP, 105, 946
Mazzotta Epifani E., Palumbo P., Capria M. T., Cremonese G., Fulle M., Colangeli L., 2007, MNRAS, 381, 713
Mazzotta Epifani E., Palumbo P., Capria M. T., Cremonese G., Fulle M., Colangeli L., 2008, MNRAS, 390, 265
Mazzotta Epifani E., Palumbo P., Capria M. T., Cremonese G., Fulle M., Colangeli L., 2009, A&A, 502, 355
Mazzotta Epifani E., Dall'Ora M., di Fabrizio L., Licandro J., Palumbo P., Colangeli L., 2010, A&A, 513, A33
Mazzotta Epifani E., Dall'Ora M., Perna D., Palumbo P., Colangeli L., 2011, MNRAS, 415, 3097
Meech K. J., Hainaut O. R., 2001, in Marov M. Y., Rickman H., eds, Collisional Processes in the Solar System. Kluwer, Dordrecht, p. 261
Meech K. J., Jewitt D. C., 1986, Icarus, 66, 561
Meech K. J., Svoren J., 2004, in Festou M. C., Keller H. U., Weaver H. A., eds, Comets II, Using Cometary Activity to Trace the Physical and Chemical Evolution of Cometary Nuclei. Univ. Arizona Press, Tucson, AZ, p. 317
Meech K. J., Weaver H. A., 1996, Earth Moon Planets, 72, 119
Meech K. J., Belton M. J. S., Mueller B. E. A., Dicksion M. W., Li H. R., 1993, AJ, 106, 1222
Meech K. J. et al., 2009, Icarus, 201, 719
Moreno F., 2009, ApJS, 183, 33
Niimi R. et al., 2012, ApJ, 744, 18
Prialnik D., 1992, ApJ, 388, 196
Probstein R. F., 1969, in Bisshopp F. et al., Problems of Hydrodynamics and Continuum Mechanics. Soc. Indust. Appl. Math., Philadelphia, PA, p. 568
Rettig T. W., Tegler S. C., Pasto D. J., Mumma M. J., 1992, ApJ, 398, 293
Russell H. N., 1916, ApJ, 43, 173
Senay M. C., Jewitt D C, 1994, Nature, 371, 229
Snodgrass C., Lowry S. C., Fitzsimmons A., 2008, MNRAS, 385, 737
Stansberry J. A. et al., 2004, ApJS, 154, 463
Szabo Gy. M., Kiss L. L., Sarneczky K., Sziladi K., 2002, A&A, 384, 702
Trigo-Rodriguez J. M., Garca-Melendo E., Davidsson B. J. R., Snchez A., Rodrguez D., Lacruz J., de Los Reyes J. A., Pastor S., 2008, A&A, 485, 599
Trigo-Rodriguez J. M., Garca-Hernndez D. A., Snchez A., Lacruz J., Davidsson B. J. R., Rodrguez D., Pastor S., de Los Reyes J. A., 2010, MNRAS, 409, 1682
Whipple F. L., 1950, ApJ, 111, 375

This paper has been typeset from a TEX/LATEX file prepared by the author.